Michaelis-Menten kinetics in shear flow: Similarity solutions for multi-step reactions

W. D. Ristenpart[1,a)] and H. A. Stone[2]
[1]*Department of Chemical Engineering and Material Science and Department of Food Science and Technology, University of California at Davis, Davis, California 95616, USA*
[2]*Department of Mechanical and Aerospace Engineering, Princeton University, Princeton, New Jersey 08544, USA*

(Received 19 September 2011; accepted 9 January 2012; published online 31 January 2012)

Models for chemical reaction kinetics typically assume well-mixed conditions, in which chemical compositions change in time but are uniform in space. In contrast, many biological and microfluidic systems of interest involve non-uniform flows where gradients in flow velocity dynamically alter the effective reaction volume. Here, we present a theoretical framework for characterizing multi-step reactions that occur when an enzyme or enzymatic substrate is released from a flat solid surface into a linear shear flow. Similarity solutions are developed for situations where the reactions are sufficiently slow compared to a convective time scale, allowing a regular perturbation approach to be employed. For the specific case of Michaelis-Menten reactions, we establish that the transversally averaged concentration of product scales with the distance x downstream as $x^{5/3}$. We generalize the analysis to n-step reactions, and we discuss the implications for designing new microfluidic kinetic assays to probe the effect of flow on biochemical processes. © *2012 American Institute of Physics*. [doi:10.1063/1.3679950]

I. INTRODUCTION

Many biochemical processes involve the interplay of diffusion, reaction, and flow. In some cases, the flow is uniform and simply advects well mixed materials from one location to another. Most biological and microfluidic systems of interest, however, do not involve uniform flows; instead, gradients in flow velocity play an active role by stretching fluid elements and increasing the effective area over which diffusion and reaction occur.[1] For example, high shear rates cause stretching of von Willibrand factor, which facilitates platelet aggregation[2] or enzymatic cleavage[3] for blood clotting. Moreover, flow in the circulatory system exerts shear stress on red blood cells and the surrounding endothelial cells, both of which can respond by releasing chemicals.[4,5] In turn, these chemicals either act as vasodilatory signaling molecules[6] or haemostatic factors, which can rapidly modify the local microenvironment by diffusion and convection and induce corresponding biological reactions, mostly via enzymatic reactions.[7] Other examples of these kinds of effects are associated with drug release from patches, such as may be used to induce blood clotting.[8] In addition, flow in the developing embryo (embryogenesis) is believed to determine the left-right body axis of a vertebrate by triggering intercellular signaling via downstream transport processes.[9] Flow can also be used to probe the kinetics of DNA conformational changes[10] or enzymatic kinetics.[11,12] Since all of the chemical processes mentioned here occur under specific flow conditions and the sites of chemical release or targeting are often fixed surfaces in the flow domain, with the chemical reactions often occurring in bulk, the temporal and spatial distributions of the chemicals, and thus the associated enzymatic kinetics, are linked directly to a shear flow.

[a)]Electronic mail: wdristenpart@ucdavis.edu.

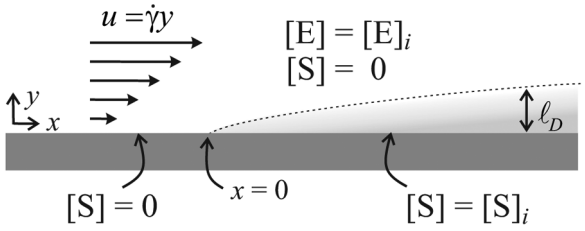

FIG. 1. Definition sketch for an enzymatic reaction in a linear shear flow. Here S denotes the substrate, E denotes the enzyme, E_i indicates the initial enzyme concentration flowing in from the left, and S_i the substrate concentration at the surface to the right of $x = 0$.

Despite the importance of this active interplay between flow, diffusion, and reaction, almost all research to date have concerned single-step surface reactions (see for example Refs. 13 or 14), and little work is available to characterize nonlinear or multi-step reactions occurring within the shear flow. Here, we present a theoretical framework for characterizing multi-step reactions that occur when an enzyme or enzymatic substrate is released from a flat solid surface into a linear shear flow (Fig. 1). Similarity solutions are developed for situations where the reactions are sufficiently slow compared to a convective time scale, allowing a regular perturbation approach to be employed. For the specific case of Michaelis-Menten reactions, we establish that the transversally averaged concentration of product scales with the distance x downstream as $x^{5/3}$. We generalize the analysis to n-step reactions, and we discuss the implications for designing new microfluidic kinetic assays to probe the effect of flow on biochemical processes.

II. THEORY

A. Michaelis-Menten kinetics

One important class of problems in chemistry and biology concerns enzymatic reactions, which most often have nonlinear kinetics and involve the interplay of two or more chemicals.[15] The most familiar case is Michaelis-Menten kinetics,[16] where the binding of a substrate (S) to an enzyme (E) first produces an intermediate (E·S) that then gives the enzyme back and yields a product (P)

$$\mathrm{E} + \mathrm{S} \underset{k_{-1}}{\overset{k_1}{\rightleftarrows}} \mathrm{E}\cdot\mathrm{S} \xrightarrow{k_2} \mathrm{E} + \mathrm{P}. \tag{1}$$

For the flow systems of interest here, we restrict attention to situations where the fluid velocity and inlet concentrations and boundary conditions are all invariant in time. In this limit, we have governing equations for each chemical species of the form

$$\mathbf{u}\cdot\nabla c_i = D_i\nabla^2 c_i + f_i(\{c_j\}), \tag{2}$$

where $\mathbf{u}$ is the velocity field, D_i is the diffusivity of species i, and $f_i(\{c_j\})$ denotes the rate of production or consumption of species i, which in general can depend on all of the concentrations of other species in a nonlinear fashion.

In systems with smallest dimension h on the order of magnitude 10–100 microns, under typical microfluidic flow conditions, the Péclet number $\mathrm{Pe} \equiv uh/D \gg 1$; for typical speeds $u = 10\,\mathrm{cm/s}$, shear rates $\dot{\gamma} = 10^3 - 10^4\mathrm{s}^{-1}$ are common.[17,18] Because the Péclet number is large, the standard boundary layer approximation applies, i.e., the x-direction (flow-direction) derivatives in the Laplacian are negligible compared to the y-direction (transverse) derivatives.[19] Then, in the case of a shear flow $u = \dot{\gamma}y$ in the x-direction (Fig. 1), the steady-state transport equations simplify for the specific case of Michaelis-Menten kinetics to

$$\dot{\gamma} y \frac{\partial [\mathrm{S}]}{\partial x} = D_S \frac{\partial^2 [\mathrm{S}]}{\partial y^2} - k_1 [\mathrm{S}][\mathrm{E}] + k_{-1} [\mathrm{E} \cdot \mathrm{S}], \tag{3a}$$

$$\dot{\gamma} y \frac{\partial [\mathrm{E}]}{\partial x} = D_E \frac{\partial^2 [\mathrm{E}]}{\partial y^2} - k_1 [\mathrm{S}][\mathrm{E}] + (k_{-1} + k_2)[\mathrm{E} \cdot \mathrm{S}], \tag{3b}$$

$$\dot{\gamma} y \frac{\partial [\mathrm{E} \cdot \mathrm{S}]}{\partial x} = D_{E \cdot S} \frac{\partial^2 [\mathrm{E} \cdot \mathrm{S}]}{\partial y^2} + k_1 [\mathrm{S}][\mathrm{E}] - (k_{-1} + k_2)[\mathrm{E} \cdot \mathrm{S}], \tag{3c}$$

$$\dot{\gamma} y \frac{\partial [\mathrm{P}]}{\partial x} = D_P \frac{\partial^2 [\mathrm{P}]}{\partial y^2} + k_2 [\mathrm{E} \cdot \mathrm{S}]. \tag{3d}$$

Note that Eqs. (3a)–(3d) are similar to the usual kinetic equations in that the left-hand side plays the role of the time derivative. The presence of the diffusive terms on the right-hand side, however, complicate matters considerably since diffusion limits the rate at which the overall chemical reaction occurs. This latter diffusive effect is ordinarily not considered since the typical bench-scale laboratory reactor is assumed well mixed; here, we focus on a parallel laminar flow design in which diffusion controls the volume where both substrate and enzyme are located.

To complete the problem statement, boundary conditions must be specified. Two important classes of boundary conditions are (1) release of a substrate from a localized part of a surface into a stream containing enzyme and (2) the inverse situation where enzyme is released into a stream containing substrate. In both situations, the effective reaction volume depends on the extent to which the enzyme or substrate diffuses into the shear flow; outside of this region, the reaction rate is zero since only one of the two reactants is present. A solution via matched asymptotic expansions is available for the case where the enzyme and intermediate diffusivities are identically zero,[20] but because Eqs. (3a)–(3d) are coupled and nonlinear, for the fully general case, one must resort to numerical methods.

Recasting the governing equations in dimensionless terms, however, aids identification of limiting cases where approximate analytical solutions are possible. We focus here on the case where substrate diffuses from the surface into the bulk where enzyme is present (Fig. 1). Choosing $\ell_D \equiv \sqrt{D_S/\dot{\gamma}}$ as a characteristic convective-diffusive length scale, we let

$$X \equiv \frac{x}{\sqrt{D_S/\dot{\gamma}}}, \quad Y \equiv \frac{y}{\sqrt{D_S/\dot{\gamma}}}, \tag{4}$$

$$S \equiv \frac{[\mathrm{S}]}{[\mathrm{S}]_i}, \quad E \equiv \frac{[\mathrm{E}]}{[\mathrm{S}]_i}, \quad E \cdot S \frac{[\mathrm{E} \cdot \mathrm{S}]}{[\mathrm{S}]_i}, \quad P \equiv \frac{[\mathrm{P}]}{[\mathrm{S}]_i},$$

where the subscript i denotes the inlet concentration. The governing equations then become

$$Y \frac{\partial S}{\partial X} = \frac{\partial^2 S}{\partial Y^2} - \varepsilon_1 SE + \varepsilon_{-1} E \cdot S, \tag{5a}$$

$$Y \frac{\partial E}{\partial X} = \delta_E \frac{\partial^2 E}{\partial Y^2} - \varepsilon_1 SE + (\varepsilon_{-1} + \varepsilon_2) E \cdot S, \tag{5b}$$

$$Y \frac{\partial E \cdot S}{\partial X} = \delta_{ES} \frac{\partial^2 E \cdot S}{\partial Y^2} + \varepsilon_1 SE - (\varepsilon_{-1} + \varepsilon_2) E \cdot S, \tag{5c}$$

$$Y \frac{\partial P}{\partial X} = \delta_P \frac{\partial^2 P}{\partial Y^2} + \varepsilon_2 E \cdot S. \tag{5d}$$

Here, we have defined the dimensionless parameters

$$\varepsilon_1 \equiv \frac{k_1[\mathrm{S}]_i}{\dot{\gamma}}, \quad \varepsilon_{-1} \equiv \frac{k_{-1}}{\dot{\gamma}}, \quad \varepsilon_2 \equiv \frac{k_2}{\dot{\gamma}}, \tag{6}$$

and δ_i is the diffusivity of species i normalized by the substrate diffusivity.

B. Similarity solution

Examination of characteristic magnitudes for the dimensionless groups motivates an analytical approximation. Enzyme and substrate concentrations are typically on the order of millimolar at most, while rate constants vary tremendously depending on the reaction but usually are in the range 10^1 to $10^7\,\mathrm{M}^{-1}\,\mathrm{s}^{-1}$. Since shear rates on the order of $\dot{\gamma} = 10^4\mathrm{s}^{-1}$ are common in microfluidic flows, the inequality

$$\varepsilon_1 = \frac{k_1[\mathrm{S}]_i}{\dot{\gamma}} \ll 1 \tag{7}$$

is satisfied easily. This dimensionless group, which is often referred to as a Dahmköhler number, gauges the relative speeds of the reaction and convection. Likewise, ϵ_{-1} and ϵ_2 are expected to be small, but the analysis here requires that they be no larger than $O(1)$. When the reaction speed is sufficiently small (i.e., the inequality in Eq. (7) is valid) and assuming there is negligible intermediate present in the inlet, then the substrate concentration evolves approximately according to

$$Y\frac{\partial S}{\partial X} = \frac{\partial^2 S}{\partial Y^2}. \tag{8}$$

Importantly, in this limit, the substrate concentration is completely decoupled from the enzyme concentration and S follows the classical (Lévêque) similarity solution.[19] Substitution of the similarity variable

$$\eta \equiv \frac{Y}{(3X)^{1/3}}, \tag{9}$$

and application of the boundary conditions

$$S = 1, \qquad \eta = 0, \tag{10a}$$

$$S \to 0, \qquad \eta \to \infty, \tag{10b}$$

yields the solution

$$S(\eta) = \frac{\int_\eta^\infty e^{-s^3/3}ds}{\int_0^\infty e^{-s^3/3}ds} = \frac{\Gamma\left(\frac{1}{3}, \frac{\eta^3}{3}\right)}{\Gamma\left(\frac{1}{3}\right)} \equiv \Psi(\eta), \tag{11}$$

where Γ denotes the Gamma function. It is straightforward to evaluate the above integrals numerically. Note that because all reaction terms have been neglected, $\Psi(\eta)$ represents the maximum possible concentration of the substrate for a given velocity field and substrate diffusivity; inclusion of reaction terms will decrease the concentration at any given location because the substrate is consumed. As for the other species, if we assume that enzyme is not consumed at the solid surface and that no intermediate or product is present at any boundaries, then in the same limit of no reaction, the concentrations are simply

$$E = \frac{[\mathrm{E}]_i}{[\mathrm{S}]_i} \equiv E_i, \quad E \cdot S = 0, \quad P = 0, \tag{12}$$

for all space.

With known concentration fields in the limit of no reaction, we now develop a perturbation solution for finite but small reaction rates, i.e., for $0 < \varepsilon_1 \ll 1$. For common microfluidic or physiological situations where there is excess of enzyme, we take $E \approx E_i$, and neglecting back reactions, which is a good approximation when the concentration of the intermediate is small, then the intermediate and product concentrations [cf. Eqs. (5c) and (5d)] evolve according to

$$Y\frac{\partial E\cdot S}{\partial X} = \delta_{E\cdot S}\frac{\partial^2 E\cdot S}{\partial Y^2} + \varepsilon_1 E_i \Psi(\eta), \tag{13a}$$

$$Y\frac{\partial P}{\partial X} = \delta_P \frac{\partial^2 P}{\partial Y^2} + \varepsilon_2 E\cdot S. \tag{13b}$$

We again substitute the similarity variable, and if we let

$$E\cdot S \equiv \varepsilon_1 E_i (3X)^{2/3}\Phi(\eta), \tag{14a}$$

$$P \equiv \varepsilon_1\varepsilon_2 E_i (3X)^{4/3}\Upsilon(\eta), \tag{14b}$$

then we obtain the system of ordinary differential equations

$$\delta_{E\cdot S}\Phi'' + \eta(\eta\Phi' - 2\Phi) + \Psi = 0, \tag{15a}$$

$$\delta_P\Upsilon'' + \eta(\eta\Upsilon' - 4\Upsilon) + \Phi = 0, \tag{15b}$$

where the primes denote differentiation with respect to η. As for boundary conditions, we require that there be zero flux of intermediate and product into the solid surface and that their concentrations vanish far from the surface, viz.,

$$\Phi' = 0, \quad \Upsilon' = 0, \quad \eta = 0, \tag{16a}$$

$$\Phi \to 0, \quad \Upsilon \to 0, \quad \eta \to \infty. \tag{16b}$$

The numerical solutions to Eqs. (15a) and (15b) are plotted in Fig. 2(a) for the case of equal diffusivities ($\delta_{E\cdot S} = \delta_P = 1$). Both Ψ and Υ are maximum at the solid surface ($\eta = 0$) and then decay to zero far away ($\eta \to \infty$). This result is physically intuitive, since the product concentrations are highest where the reactant concentration is largest, i.e., near the surface. An example of the effect of unequal diffusivities is shown in Fig. 2(b). Since enzymes are typically much larger than the substrate, while the product is of comparable size to the substrate, we

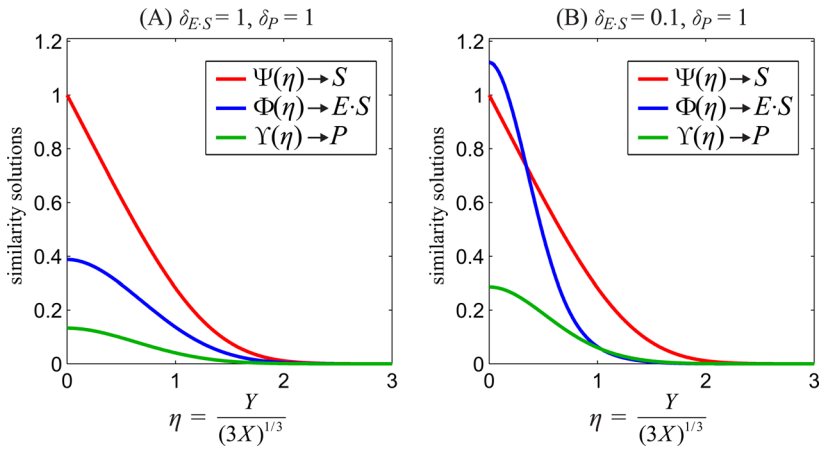

FIG. 2. The similarity solutions for the various concentration fields for (A) equal diffusivities and (B) unequal diffusivities.

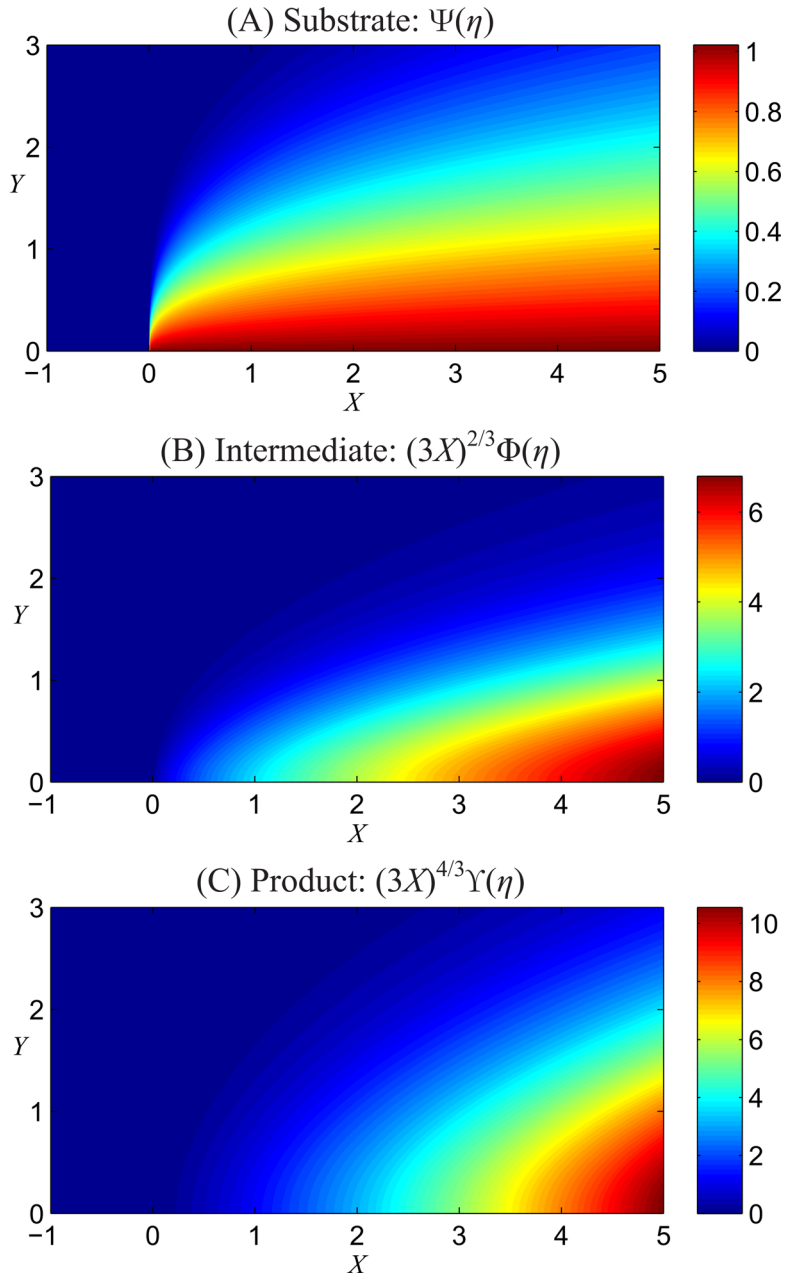

FIG. 3. Contour plots of the dimensionless concentration fields for the case $\delta_{E\cdot S} = 0.1$, $\delta_P = 1$.

choose $\delta_{E\cdot S} = 0.1$ and $\delta_P = 1$ as representative diffusivities. The primary effects of a smaller intermediate diffusivity are that the concentration of intermediate and product are both noticeably increased near the solid surface while decaying more rapidly with distance. The decreased diffusivity tends to "confine" any formed intermediate near the solid surface.

A perhaps more intuitive visualization of the similarity solution is shown in Fig. 3, which shows contour plots of the scaled concentration fields in X-Y space. The substrate concentration follows the standard Lévêque behavior: the concentration is uniform along the surface for $X > 0$ and decays into the bulk, with a sharp discontinuity at $X = 0$. In contrast, the concentration of the intermediate and product both increase with X, *albeit* at different rates; consistent with the reaction scheme, the intermediate forms earlier (i.e., at smaller values of X). For this specific

example, the intermediate diffusivity is smaller, and accordingly, the intermediate penetrates a smaller distance into the bulk flow.

In many experimental situations where concentrations are indicated by fluorescence[21–24] or photoluminescence,[25–27] it is common to measure the light emitted from the projected area rather than individual points. In this case, a convenient measure of the effective concentration is obtained by integrating the concentration in the y-direction to arrive at the area-averaged concentration, which varies in the x-direction, i.e.,

$$\langle E \cdot S \rangle \equiv \int_0^\infty [E \cdot S] dy = \varepsilon_1 \ell_D [E]_i (3X) \int_0^\infty \Psi(\eta) d\eta. \tag{17}$$

Note that an extra factor of $(3X)^{1/3}$ results from the change of variables. Likewise, for the product we have

$$\langle P \rangle \equiv \int_0^\infty [P] dY = \varepsilon_1 \varepsilon_2 \ell_D [E]_i (3X)^{5/3} \int_0^\infty \Upsilon(\eta) d\eta, \tag{18}$$

or, in fully dimensional terms,

$$\langle E \cdot S \rangle = a_\delta \frac{k_1 [S]_i [E]_i}{\dot{\gamma}} x, \tag{19a}$$

$$\langle P \rangle = b_\delta \frac{k_1 k_2 [S]_i [E]_i}{D_S^{1/3} \dot{\gamma}^{5/3}} x^{5/3}. \tag{19b}$$

Here, a_δ and b_δ are dimensionless constants defined as

$$a_\delta \equiv 3 \int_0^\infty \Psi(\eta) d\eta, \quad b_\delta \equiv 3^{5/3} \int_0^\infty \Upsilon(\eta) d\eta, \tag{20}$$

which depend only on the relative magnitudes of the species diffusivities. Numerical quadrature of the similarity solutions shows that both a_δ and b_δ depend very weakly on the species

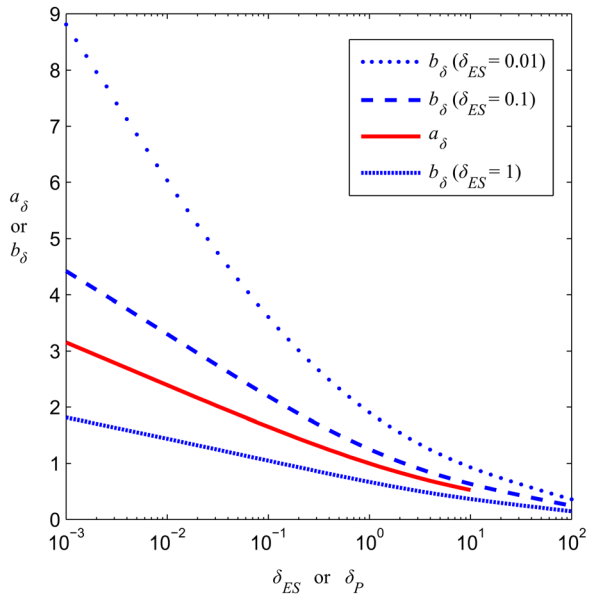

FIG. 4. Magnitude of the prefactor a_δ as a function of δ_{ES} and magnitude of the prefactor b_δ as a function of δ_P for three different values of δ_{ES}; cf. Eq. (20).

diffusivities, ranging at most between approximately 0.5 to 9 over five orders of magnitude in the relative diffusivities (Fig. 4).

C. Generalization to n-step reactions

The preceding similarity scheme can be generalized to multi-step reactions with an arbitrary number of intermediate species, i.e., reactions of the form

$$\mathrm{E} + \mathrm{S} \xrightarrow{k_1} \mathrm{I}_1 \xrightarrow{k_2} \mathrm{I}_2 \cdots \xrightarrow{k_{n-1}} \mathrm{I}_{n-1} \xrightarrow{k_n} \mathrm{P}. \tag{21}$$

Here, I_j represents the jth intermediate species and all rate coefficients k_j are first order with the exception of k_1. For simplicity, we omit any back reactions. Note that the previous Michaelis-Menten scheme is recovered by letting $n=2$ and identifying I_1 as E·S. We again restrict attention to situations where the Péclet number is large and where all reaction time scales are slow compared to the convective time scale, i.e., $k_j/\dot{\gamma} \ll 1$ for all j. Likewise, we restrict attention to the initial region where back reactions are negligible and where either the enzyme (or substrate) is in great excess. When these criteria are met, the perturbation scheme is simply repeated n times, and it is straightforward to demonstrate that substitution of the similarity variables

$$I_j \equiv \varepsilon_1 \varepsilon_2 \cdots \varepsilon_j E_i (3X)^{2j/3} \Phi_j(\eta), \tag{22a}$$

$$P \equiv \varepsilon_1 \varepsilon_2 \cdots \varepsilon_n E_i (3X)^{2n/3} \Upsilon(\eta), \tag{22b}$$

yields a system of coupled ordinary differential equations of the form

$$\delta_{I_1} \Phi''_1 + \eta(\eta \Phi'_1 - 2\Phi_1) + \Psi = 0, \tag{23a}$$

$$\delta_{I_j} \Phi''_j + \eta(\eta \Phi'_j - 2j\Phi_j) + \Phi_{j-1} = 0, \tag{23b}$$

$$\delta_P \Upsilon'' + \eta(\eta \Upsilon' - 2n\Upsilon) + \Phi_{n-1} = 0. \tag{23c}$$

Equation (23b) is valid for $j \geq 2$. As before, the solutions depend only on the relative magnitudes of the species diffusivities and are readily solved numerically. Perhaps of most interest is the scaling prediction for the integrated concentration, which for the product is

$$\langle P \rangle = c_\delta \frac{k_1 k_2 \cdots k_n [S]_i [E]_i}{D_S^{\frac{n-1}{3}} \dot{\gamma}^{\frac{2n+1}{3}}} x^{\frac{2n+1}{3}}. \tag{24}$$

where c_δ is a prefactor defined in a fashion similar to b_δ [cf. Eq. (20)].

III. DISCUSSION AND CONCLUSIONS

One of the key results of this analysis is Eq. (19b), which predicts that the transversally averaged concentration of product resulting from a Michaelis-Menten reaction will increase with distance downstream as $x^{5/3}$. Provided the reaction rate is sufficiently slow and the shear rate sufficiently high (so that Eq. (7) is satisfied), information about either the rate constants or the reactant concentrations could be extracted from measurements of the product concentration as a function of distance along a channel. A similar methodology has been employed for co-flow microfluidic networks where reactants are brought together in two converging channels,[25,28] but the present results provide a method for assessing situations where a reactant is released from a solid surface. Equation (19b) also predicts that the projected product concentration is highly sensitive to the imposed shear rate, i.e., $\langle P \rangle \propto \dot{\gamma}^{-5/3}$. For situations where it is inconvenient to probe multiple positions along a microchannel, an alternative approach would be to measure the product concentration at a fixed location while varying the imposed flow rate.

An especially intriguing possibility involves multi-step reactions where the exact number of intermediate species is unknown. Notably, the generalization of the similarity solution to an n-step reaction indicates that the product concentration is extremely sensitive to n (cf. Eq. (24)). As an example, for a three-step reaction, the product concentration increases as $x^{7/3}$, while for a four-step reaction, it increases as x^3. The significant difference in the power law suggests that the number of steps in an unknown reaction mechanism could be probed by measuring the product concentration versus position (or alternatively, versus different flow rates for fixed position).

The similarity solution presented here is valid in the limit of "slow" kinetics with negligible back reactions, so more detailed numerical calculations are necessary to describe systems with faster kinetics or significant back reactions. Likewise, the similarity solution also assumes a linear shear flow, whereas in many pressure-driven microfluidic situations, the flow is parabolic. More detailed calculations are necessary if the effective reaction zone extends significantly past the region of linear shear near the solid surface, or if the substrate is released within the entrance region of a microchannel where the linear shear profile is not fully developed. Moreover, in many biological situations of interest, the amount of reactant released at a liquid/cell interface actually depends on the imposed shear rate.[5] The solution presented here will serve as a limiting case for consideration of these more complicated effects.

ACKNOWLEDGMENTS

We thank Jiandi Wan for helpful conversations.

[1]J. M. Ottino, *The Kinematics of Mixing: Stretching, Chaos and Transport* (Cambridge University Press, Cambridge, UK, 1989).
[2]S. W. Schneider, S. Nuschele, A. Wixforth, C. Gorzelanny, A. Alexander-Katz, R. R. Netz, and M. F. Schneider, Proc. Natl. Acad. Sci. U.S.A. **104**, 7899 (2007).
[3]A. Bernardo, C. Ball, L. Nolasco, J. F. Moake, and J. F. Dong, Blood **104**, 100 (2004).
[4]R. S. Sprague, M. L. Ellsworth, A. H. Stephenson, and A. J. Lonigro, Am. J. Physiol. Heart Circ. Physiol. **40**, H2717 (1996).
[5]P. F. Davies, K. A. Barbee, M. V. Volin, A. Robotewskyj, J. Chen, L. Joseph, M. L. Griem, M. N. Wernick, E. Jacobs, D. C. Polacek, N. DePaola, and A. I. Barakat, Annu. Rev. Physiol. **59**, 527 (1997).
[6]R. Sprung, R. Sprague, and D. Spence, Anal. Chem. **74**, 2274 (2002).
[7]Y. H. Datta and B. M. Ewenstein, Thromb. Haemostasis **86**, 1148 (2001).
[8]C. J. Kastrup, F. Shen, M. K. Runyon, and R. F. Ismagilov, Biophys. J. **93**, 2969 (2007).
[9]A. Schweickert, T. Weber, T. Beyer, P. Vick, S. Bogusch, K. Feistel, and M. Blum, Curr. Biol. **17**, 60 (2007).
[10]G. Luo, M. Wang, W. H. Konigsberg, and X. S. Xie, Proc. Natl. Acad. Sci. U.S.A. **104**, 12610 (2007).
[11]G. H. Seong, J. Heo, and R. M. Crooks, Anal. Chem. **75**, 3161 (2003).
[12]M. B. Kerby, R. S. Legge, and A. Tripathi, Anal. Chem. **78**, 8273 (2006).
[13]T. Gervais and K. F. Jensen, Chem. Eng. Sci. **61**, 1102 (2006).
[14]T. M. Squires, R. J. Messinger, and S. R. Manalis, Nat. Biotechnol. **26**, 417 (2008).
[15]A. Fersht, *Structure and Mechanism in Protein Science: A Guide to Enzyme Catalysis and Protein Folding* (Freeman, San Francisco 1998).
[16]L. Michaelis and M. L. Menten, Biochem. Z. **49**, 333 (1913).
[17]H. A. Stone, A. D. Stroock, and A. Ajdari, Annu. Rev. Fluid Mech. **36**, 381 (2004).
[18]T. M. Squires and S. R. Quake, Rev. Mod. Phys. **77**, 977 (2005).
[19]W. M. Deen, *Analysis of Transport Phenomena* (Oxford University Press, New York, 1998).
[20]A. C. Fowler, SIAM J. Appl. Math. **33**, 289 (1977).
[21]R. F. Ismagilov, A. D. Stroock, P. J. A. Kenis, G. Whitesides, and H. A. Stone, Appl. Phys. Lett. **76**, 2376 (2000).
[22]A. E. Kamholz, E. A. Schilling, and P. Yager, Biophys. J. **80**, 1967 (2001).
[23]R. K. P. Benninger, O. Hofmann, B. Onfelt, I. Munro, C. Dunsby, D. M. Davis, M. A. A. Neil, P. M. W. French, and A. J. de Mello, Angew. Chem., Int. Ed. **46**, 2228 (2007).
[24]J. B. Salmon and A. Ajdari, J. Appl. Phys. **101**, 074902 (2007).
[25]W. D. Ristenpart, J. D. Wan, and H. A. Stone, Anal. Chem. **80**, 3270 (2008).
[26]J. D. Wan, W. D. Ristenpart, and H. A. Stone, Proc. Natl. Acad. Sci. U.S.A. **105**, 16432 (2008).
[27]A. M. Forsyth, J. D. Wan, P. D. Owrutsky, M. Abkarian, and H. A. Stone, Proc. Natl. Acad. Sci. U.S.A. **108**, 10986 (2011).
[28]J. B. Salmon, A. Ajdari, P. Tabeling, L. Servant, D. Talaga, and M. Joanicot, Appl. Phys. Lett. **86**, 094106 (2005).